Nuclear Science & Technology Research Institute

Journal of Nuclear Research and Applications

Research Paper

Journal homepage: https://jonra.nstri.ir

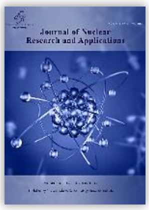


# Analysis of the Microscopic Details and Components of the Nuclear Fission for Protactinium-231

M. Sepiani [1*], M. Nasri Nasrabadi [1,2]

[1] Faculty of Physics, University of Isfahan, Hezar Gerib Ave., 81746-73441, Isfahan, Iran.
[2] Frank Laboratory of Neutron Physics, Joint Institute for Nuclear Research, 141980 Dubna, Russia.

(Received: 3 August 2024, Revised: 29 September 2024, Accepted: 9 October 2024)

**A B S T R A C T**

The nuclear fission of protactinium nuclei is a complex process influenced by an intricate interplay of nuclear components and microscopic details. This study presents a comprehensive analysis of the fission mechanism for $^{231\text{-}232}$Pa, emphasizing the role of parameters of fission barriers, static and dynamic deformations, predictions of nuclear level densities (NLD) models at the fission saddle points, and its change compared to the ground state, fission models and fission dynamics. Through a combination of theoretical modeling and advanced simulation techniques using nuclear reaction and evaporation codes, the neutron-induced fission cross sections of $^{231}$Pa are calculated and the profound impact of NLD on the static and dynamic deformations is illustrated. Our findings can be confirmed with experimental data which serve as benchmarks for the veracity of the proposed models. It is shown that the NLDs at saddle points have a significant effect on reaction results and fission path determination. Additionally, the impact of nuclear dynamic deformations should be included in the nuclear level density on the fission barriers so that the modeling can reproduce the experimental data. This study can be considered an essential roadmap for understanding the behavior of nuclear reactors and the development of nuclear energy.

***Keywords:*** Nuclear fission; Nuclear level density; Fission barriers; 231-Protactinium.

## 1. Introductions

The multifaceted nature of neutron-induced competitive nuclear fission encapsulates a treasured yet intricate dynamical phenomenon that holds considerable significance in both fundamental physics and applied nuclear technology. It provides an exceptional window into the interplays between microscopic particle interactions and macroscopic statistical processes that govern the stability and eventual division of an atomic nucleus. This research

*Corresponding Author E-mail: m.sepiani@cfu.ac.ir

DOI: https://doi.org/10.24200/jonra.2024.1630.1135.

delves into the core components critical to explicating neutron-induced competitive nuclear fission, with a concentrated focus on $^{231}$Pa as an isotope whose fission characteristics lead to significant implications for both advanced reactor technology and nuclear waste transmutation. $^{231}$Pa is a member of the uranium decay series and possesses characteristics that make it interesting for fission studies. Specifically, it serves as a potential intermediate in the production of other actinides, such as $^{233}$U, which is a key isotope in the thorium fuel cycle [1,2]. Additionally, several references have shown that $^{231}$Pa can be utilized as a burnable neutron absorber in fusion reactors [3,4]. By breeding $^{231}$Pa in these reactors and then using it in nuclear power reactors, it is possible to significantly enhance fuel burn-up. This makes $^{231}$Pa a novel and unique material for improving the efficiency of nuclear fuel cycles, a role that has not been suggested for any other isotope before. Numerous studies have focused on nuclear fission, particularly in the actinide series, but fewer studies have specifically focused on $^{231}$Pa, making it a relatively unexplored isotope in fission research. Existing research, mostly experimental, suggests that the fission properties of $^{231}$Pa may differ from other actinides, thus requiring more detailed microscopic analysis [5-7]. The intricacy of nuclear fission unfolds from the multifaceted interplay between neutrons and the target nucleus, where the formation of a compound nucleus and its subsequent passage over the fission barrier entail a sophisticated sequence of quantum and thermodynamic events. The study of $^{231}$Pa fission presents an exceptional opportunity to deepen our understanding of nuclear processes due to its unique position away from the beta-stability line, thereby challenging existing theoretical models. This research endeavors to dissect the intricacies of $^{231}$Pa fission through advanced nuclear reaction codes and theoretical modeling, primarily focusing on the nuclear level density (NLD) at the ground state and at the saddle point which is the position where the nucleus contorts into a potential energy state favorable for fission. Our analysis quantitatively distinguishes the disparity in NLD between these two crucial stages, shedding light on its implications for the fission process. A pivotal focus is placed on the effects that dynamic (shapes and vibrations that occur during the fission process) and static deformations (inherent shapes at equilibrium) have on the NLD, thereby expanding our understanding of the microscopic origins of nuclear properties. Furthermore, this study rigorously evaluates the interaction between the NLD and the barrier parameters in shaping the fission cross-section calculations, challenging existing predictive capabilities. The NLD represents a cornerstone for characterizing the fission landscape; thus, our investigation delineates the stark contrast in NLD between the ground state and the saddle point. Key hypotheses suggest that dynamic and static deformations play a pivotal role in the modulation of NLD which affects the perceived energy barriers that govern the likelihood of fission. In tandem with these deformations, this study carefully analyzes the concomitant effects on fission cross-section calculations, which are heavily influenced by both NLD and the characteristic parameters of barrier heights and curvatures. Many theoretical models have been developed that investigate NLD and its related parameters under different conditions [8-26]. Several well-known and widely used models are used in reaction codes including the phenomenological models (the constant temperature model (CTM) [8], the back-shifted Fermi gas model (BFM) [9] and the Generalized superfluid model (GSM) [27]) and the microscopic models [28-33]. We explore NLD models to ascertain the degree to which various theoretical approaches can replicate experimental observations. The fission barrier parameters (height and curvature) are amongst the most complicated aspects influencing fission probabilities. These barrier parameters directly correlate with the likelihood of the nucleus to undergo fission upon neutron absorption, thus playing an indispensable role in the estimation of fission probabilities. This comprehensive investigation elucidates the sophistication imbued within the fission of $^{231}$Pa, highlighting the pivotal effects of NLD variation from ground state to saddle point, accompanied by the critical influence of barrier parameters. This research not only represents a significant stride in understanding neutron-induced fission mechanisms but also exemplifies the symbiotic relationship between advanced theoretical frameworks and practical applications in nuclear science. It is shown that the use of different NLD models has a significant effect on the calculation of the competitive fission cross-section, and the NLD at the saddle points can have a very different behavior compared to the ground state. The behavior of NLD at the saddle points depends on the dynamic deformation of nucleus and how to account for collective and shell effects.

## 2. Key components of competitive fission

When a neutron collides with a target nucleus, it may be absorbed, leading to the creation of a compound nucleus in an excited state. The compound nucleus then undergoes de-excitation through various competitive channels, including gamma or particle emissions and fission. At low excitation energies, the fission process occurs relatively slowly and competes with the evaporation processes from the compound nucleus, which are studied by the Hauser-Feshbach formalism [34].

In this formalism, the decay probability through channel β is obtained from the ratio of the transmission coefficient of channel β to the sum of the transmission coefficients of all channels $(P_\beta = T_\beta / \sum T_\gamma)$. The fission channel is distinct from other channels because it is not directly related to the remaining nuclei of the compound nucleus that has undergone fission. The phase space of the final products has no effect on the reaction when the decision to split is made. Therefore, for a given compound nucleus energy level $J_{CN}^{\pi_{CN}}$, there is only one fission transmission coefficient.

In some models that describe the fission of heavy nuclei (transition state model), the NLD of the fissile nucleus on the fission barriers (density of transition states) and the height and shape of the fission barrier play a crucial role in determining the probability of this channel. The fission transmission coefficient is usually calculated using the Hill-Wheeler model and based on the transition state model proposed by Bohr [35,36]. The Hill-Wheeler expression determines the probability of quantum tunneling through a barrier with height $B_f$ and width $\hbar\omega_f$ for a compound nucleus with excitation energy $E^*_{CN}$.

$$T_f^{HW}(E^*_{CN}) = \frac{1}{1+\exp\left[-2\pi\frac{(E^*_{CN}-B_f)}{\hbar\omega_f}\right]} \quad (1)$$

In the transition state model shown in Fig.1, the fission process occurs through intermediate states of the compound nucleus, and the probability of fission is determined by the density of these intermediate levels. The ground state excitation energy of the nucleus expressed as a function of deformation shows a bump which is the ground state barrier. On top of this barrier, there may be several levels of the compound nucleus, and a fission barrier is assigned to each of these levels, which are called transition states. In the first-order approximation, the barrier of transition states is equal to the barrier of the ground state, which is shifted by the energy of the transition states relative to the peak of the barrier of the ground state. The transmission coefficient for a transition state with excitation energy $\varepsilon_i$ above the peak of the fission barrier *i* becomes0 [37]:

$$T_f^{HW}(E^*_{CN},\varepsilon_i) = \frac{1}{1+\exp\left[-2\pi\frac{(E^*_{CN}-B_f-\varepsilon_i)}{\hbar\omega_f}\right]} \quad (2)$$

For a compound nucleus with a specific spin and parity $J^{\pi_{CN}}_{CN}$, all fission barriers associated with transition states having that same spin and parity $J^{\pi_{CN}}_{CN}$ will play a role in the fission process. Therefore, the total fission transmission coefficient is equal to the sum of the individual fission coefficients for each barrier that could potentially be tunneled through:

$$T_f^{J^{\pi CN}_{CN}}(E^*_{CN}) = \sum_i T_f^{HW}(E^*_{CN}).\delta(i,J^{\pi_{CN}}_{CN}) + \int_{E_{Th}}^{E^*_{CN}} \rho_f(\varepsilon,J_{CN},\pi_{CN}).T_f^{HW}(E^*_{CN},\varepsilon).d\varepsilon \quad (3)$$

Where $\rho_f(\varepsilon,J_{CN},\pi_{CN})$ is the fission NLD (density of transition states) in the deformation of the fission saddle point. In this expression, if the spin and parity of the transition state are the same as the compound nucleus, then $\delta(i,J^{\pi_{CN}}_{CN})=1$ and otherwise, $\delta(i,J^{\pi_{CN}}_{CN})=0$.

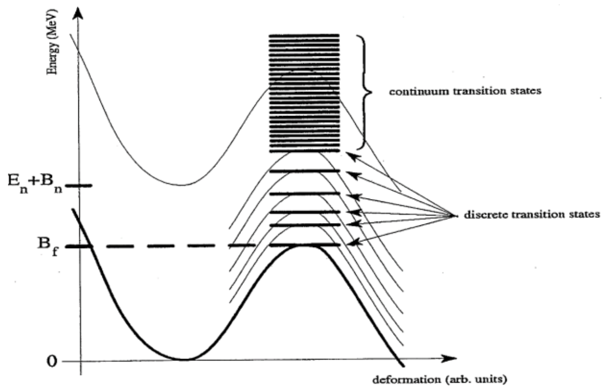


**Fig. 1**. Potential energy as a function of deformation for a single-humped barrier [37, 38].

As shown in Fig. 2, in many cases (especially in the mass region of actinides), multi-humped fission barriers (two or three peaks) are observed, which must be crossed in addition to the first barrier for fission to occur. The change in the shape of the fission barriers compared to the prediction of the liquid drop model (LD) and the creation of these multi-humped barriers is due to the application of shell effects (SM). Usually, a simple approximation can be sufficient to solve the multi-humped barriers problem.

In the case of double-humped barriers, first, the fission transmission coefficients for each of the fission barrier A and Bare calculated. Then it is assumed that it is possible to separate the tunneling process through these two barriers (such as the formation and decay of the compound nucleus) and express it as two separate stages (independence hypothesis). In this regard, we calculate the probability of crossing the first barrier $T_A$, and then we multiply it by the probability of splitting. Once the first barrier is crossed, there are two possibilities: either crossing the barrier A and turning back with probability $T_A$, or splitting through the barrier B with probability $T_B$. Therefore, as in the case of the probability of decay into an exit channel $(P_\beta = T_\beta / \sum T_\gamma)$, it is obvious that the probability of splitting after passing the first barrier will be:

$$P_{\text{fission}} = \frac{T_B}{T_A + T_B} \tag{4}$$

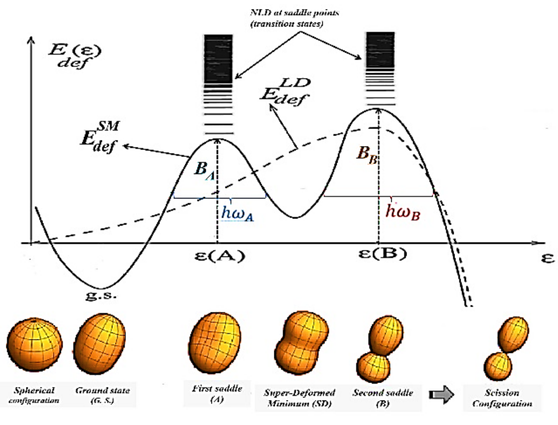


**Fig. 2**. Potential energy as a function of deformation (double-humped barriers) and fission dynamic [37, 38].

As a result, the effective fission transmission coefficient for the double-humped barriers is:

$$T_{\text{eff}}^{J_{CN}^{\pi CN}} = \frac{T_A^{J_{CN}^{\pi CN}} . T_B^{J_{CN}^{\pi CN}}}{T_A^{J_{CN}^{\pi CN}} + T_B^{J_{CN}^{\pi CN}}} \tag{5}$$

In the case of the three-humped barriers, using the independence hypothesis leads to the following effective transmission coefficient:

$$T_{\text{eff}}^{J_{CN}^{\pi CN}} = \frac{T_{AB}^{J_{CN}^{\pi CN}} . T_C^{J_{CN}^{\pi CN}}}{T_{AB}^{J_{CN}^{\pi CN}} + T_C^{J_{CN}^{\pi CN}}} \tag{6}$$

where, $T_{AB}^{J_{CN}^{\pi CN}}$ is the previous transmission coefficient of the double barrier.

## 3. Fission level density

The nuclear level density (NLD) of a fissile nucleus is related to the deformation of the fission saddle point and the parameters of the fission barrier. In deformed nuclei, the effects of deformation, shell, and pairing correlations play a significant role in the NLD. Phenomenological NLD models, based on the Fermi gas model, do not consider the effects of deformation. However, collective effects due to deformation are incorporated into NLD both explicitly and implicitly. Explicitly, collective effects are included as multiplying factors in the intrinsic NLD.

$$\rho_{\text{def}}(E_x, J, \pi) = K_{\text{Rot}}(E_x, J)\rho_{\text{int}}(E_x, J, \pi) \tag{7}$$

where collective rotational factor is $K_{\text{Rot}} = \sigma^2_{\text{cut-off}\perp} = 0.01389 A^{5/3}(1 + \beta_2/3)\sqrt{E_{ex}/a}$ for ground state deformation and axially symmetric nuclei. $K_{Rot}$ for barriers depends on the type of symmetry or asymmetry of barriers. For axially asymmetric in barriers:

$$K_{\text{Rot}} = \left[\sqrt{\frac{\pi}{2}}\sigma^2_{\text{cut-off}\perp}(1 + 2\beta_2/3)\sigma^2_{\text{cut-off}\|} - 1\right] f(E_{ex}) + 1 \tag{8}$$

where $\sigma^2_{cut-off\|} = 0.01389A^{5/3}\sqrt{aE_{ex}}/\tilde{a}$ and $f(E_{ex}) = 1/\left(1+\exp\left(E_{ex}-E^{bar}_{col}/d^{bar}_{col}\right)\right)$ are parallel spin cut off parameter and a combination of Fermi functions (where $E^{bar}_{col} = 45\text{MeV}, d^{bar}_{col} = 5\text{MeV}$), respectively. In the implicit (effective) way, the effective NLD parameter (NLDP) is calculated for each saddle point. All phenomenological models of NLD at energies higher than a few MeV (after matching energy $E_M$) use the well-known Fermi gas relation [10]:

$$\rho_{FG}(U) = \frac{\sqrt{\pi}}{12}\frac{e^{2\sqrt{aU}}}{a^{1/4}U^{5/4}} \tag{9}$$

where *a* is energy-dependent NLDP (to account for shell effects) [39-41]:

$$a(E_{ex}) = \tilde{a}\left(1+\delta W\frac{1-\exp(-\gamma E_{ex})}{E_{ex}}\right) \tag{10}$$

where $\delta W$ is the shell correction energy and damping function of shell effects is $1-\exp(-\gamma E_{ex})/E_{ex}$ and the damping parameter ($\gamma$) determines the rate of approach of $a(E_x)$ to $\tilde{a} = \alpha A + \beta A^{2/3}$ ($\alpha$&$\beta$&$\gamma$ are global parameters [42]). The effective asymptotic NLDP for fission barrier is expressed as [37, 43]:

$$\begin{aligned} \tilde{a}^{eff} &= \frac{A}{13}f(E_{ex}) + \tilde{a}(1-f(E_{ex})), \\ f(E_{ex}) &= 1/\left[1+\exp-\left(\left(E_{ex}-E^{bar}_{col}\right)/d^{bar}_{col}\right)\right] \end{aligned} \tag{11}$$

Where $E^{bar}_{col} = 30\text{MeV}, d^{bar}_{col} = 5\text{MeV}$ [37].

## 4. Results and discussion

Here, the cross section of the 231Pa fission reaction induced by neutrons is calculated using the TALYS nuclear reaction code (37) and all phenomenological and microscopic models of NLD without collective effects. The results of these calculations are then compared with experimental data, as shown in Fig. 3.

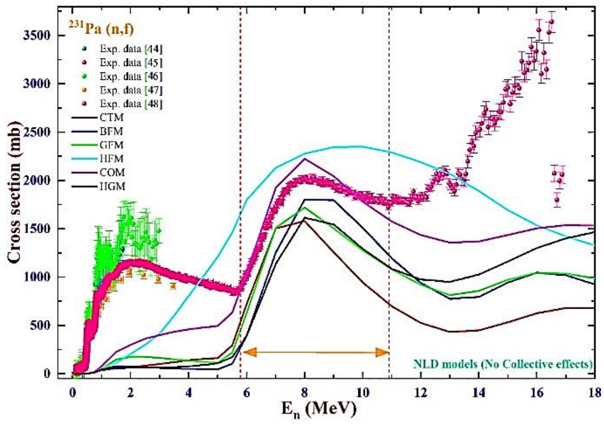


**Fig. 3**. Comparison of fission cross section calculations using various NLD model (without collective effects) and experimental data [44-48].

It is evident that utilizing different NLD models greatly influences the calculation results. Furthermore, these models, when not taking into account the collective effect, are unable to accurately replicate the experimental data, except within the 6 to 11 MeV range. Therefore, it is crucial to make adjustments to incorporate the effects of deformation and collective excitations in the NLD, along with its effective parameters and the parameters of fission barriers. The outcomes of these modifications, as depicted in Fig. 4, demonstrate that these microscopic intricacies in the fission process can have a significant impact and improve the quality of reproducing the fission cross-section.

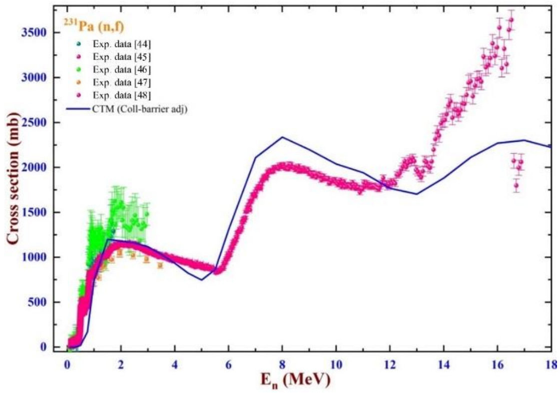


**Fig. 4**. Fission cross section calculations using adjusted CTM NLD model with collective effects and adjusted barrier parameters.

The parameters for the microscopic details of the $^{231}$Pa(n,f) reaction, including NLD parameters such as the CTM model: matching energy ($E_M$), T and $E_0$ parameters, effective asymptotic NLDP, spin cutoff parameters, Ignatyuk relation parameters at saddle points) and fission barrier parameters (curvature and height), are provided to calculate the fission cross section. These parameters are shown in Table 1. As shown in Table 1 and Fig. 4, many parameters of the CTM model of nuclear level density in the ground state and on the inner and outer fission barriers have different values. This difference is due to the dynamic deformation of the nucleus compared to the deformation of its ground state during the fission process. In this investigation, the role of collective effects (rotational and vibrational) caused by this deformation on NLD is significant. By considering these effects in the calculations and adjusting other NLD parameters, the results of the calculations and simulations can be brought closer to the experimental values to a great extent. Determining and investigating how each component changes during the dynamic fission reaction is still one of the challenging issues in nuclear physics and technology. Itis being developed along with the improvement of laboratory methods.

**Table 1.** The parameters of microscopic details of $^{231}$Pa(n,f) reaction for each barriers.

| Nuclei | Barrier | $a^{eff}$ | T | $E_0$ | $E_M$ | δW | $B_f$ | hω | Barrier axiality |
|---|---|---|---|---|---|---|---|---|---|
| $^{232}$Pa | inner | 28.18818 | 0.32817 | -0.87829 | 2.07533 | 1.98466 | 5.0 | 0.60 | axially symmetric |
| | outer | 30.95610 | 0.53817 | -3.76143 | 3.76052 | 3.78528 | 6.2 | 0.40 | tri-axial |
| $^{231}$Pa | inner | 28.16833 | 0.38172 | -1.11469 | 4.91575 | 2.07699 | 5.5 | 1.0 | axially symmetric |
| | outer | 28.16833 | 0.40368 | -0.85178 | 4.55453 | 2.07699 | 5.5 | 0.5 | tri-axial |

## 5. Conclusions

In this study, we investigated the microscopic details and components of nuclear fission for protactinium nuclei. We calculated the neutron-induced fission cross section for the 231Pa nucleus by determining the nuclear level density parameters at the saddle points on the fission barriers, as well as the shape and parameters of the fission barriers (height and curvature). Additionally, we obtained optimized values for the microscopic details of competitive fission. The effect of dynamic deformation by shape-dependent rotational enhancements was also considered in the NLD. Our findings revealed that different nuclear level density models have a significant impact on the results of the competitive fission reaction. It was also demonstrated that the parameters of the NLD on the fission barriers differ significantly from the ground state, highlighting the importance of accurate determination for precise nuclear fission prediction. This information provides crucial insights into the dynamics and behavior of the nucleus during the fission process. Our results indicate that incorporating dynamic deformation effects in the NLD results in a substantial increase in the calculated fission cross section. Furthermore, different nuclear level density models significantly influence the results of the competitive fission reaction due to variations in level density values at the saddle points, impacting the calculated fission cross section. These findings are essential for comprehending the dynamics of nuclear fission. In conclusion, accurate determination of fission barriers and nuclear level density parameters is crucial for predicting the fission cross section accurately. This knowledge can be utilized to enhance nuclear models and design more efficient nuclear reactors.

## Conflict of interest

The authors declare no potential conflict of interest regarding the publication of this work.

## References


[1] Maslov VM, Baba M, Hasegawa A, Kornilov NV, Kagalenko AB, Tetereva NA, editors. 231Pa and 233Pa Neutron-Induced Fission Data Analysis. AIP Conference Proceedings; 2005: American Institute of Physics.

[2] Shmelev AN, Kulikov GG, Kulikov EG, Apse VA. Protactinium-231 as a new fissionable material for nuclear reactors that can produce nuclear fuel with stable neutron-multiplying properties. Kerntechnik. 2016;81(1):34-7.

[3] Kulikov G, Kulikov E, Shmelev A, Apse V. Protactinium-231–New burnable neutron absorber. Nuclear Energy and Technology. 2017;3(4):255-9.

[4] Imamura T, Saito M, Yoshida T, Artisyuk V. Potential of 231Pa for gas cooled long-life core. Journal of nuclear science and technology. 2002;39(3):226-33.

[5] Maslov V, editor Protactinium neutron-induced fission up to 200 MeV. EPJ Web of Conferences; 2010: EDP Sciences.

[6] Kemmer J, Kim J, Born H-J. Study on the Reactor Neutron-induced Fission of 231Pa. Radiochimica Acta. 1970;13(4):181-228.

[7] Kobayashi K, Yamamoto S, Lee S, Cho H-J, Yamana H, Moriyama H, et al. Measurement of neutron-induced fission cross sections of 229Th and 231Pa using linac-driven lead slowing-down spectrometer. Nuclear science and engineering. 2001;139(3):273-81.

[8] Gilbert A, Cameron A. A composite nuclear-level density formula with shell corrections. Canadian Journal of Physics. 1965;43(8):1446-96.

[9] Dilg W, Schantl W, Vonach H, Uhl M. Level density parameters for the back-shifted fermi gas model in the mass range 40< A< 250. Nuclear Physics A. 1973;217(2):269-98.

[10] Bethe H. An attempt to calculate the number of energy levels of a heavy nucleus. Physical Review. 1936;50(4):332.

[11] Nasrabadi MN, Sepiani M. Generalization of phenomenological models of nuclear level density to high energies. Physica Scripta. 2015;90(12).

[12] Aggarwal M. Dependence of spin induced structural transitions on level density and neutron emission spectra. Nuclear Physics A. 2019;983:166-74.

[13] Agrawal BK, Ansari A. Level density and level density parameter in medium heavy nuclei including thermal and quantal fluctuation effects. Physics Letters B. 1998;421(1):13-7.

[14] Canuto V, Fassio L, Rojo O. Statistical mechanics of a superfluid nuclear matter: (II). Nuclear level density. Nuclear Physics A. 1967;97(1):223-31.

[15] Canuto V, Garcia-Colin LS. Odd-even effect in the nuclear level density and superfluid model of nuclei. Nuclear Physics. 1965;61(2):177-93.

[16] Ingeberg VW, Jones P, Msebi L, Siem S, Wiedeking M, Aungwa A, et al. Nuclear Level Density and $\gamma$-ray Strength Function of $^{63}\mathrm{Ni}$2022 July 01, 2022:[arXiv:2207.01571 p.]. Available from: https://ui.adsabs.harvard.edu/abs/2022arXiv220701571I.

[17] Nasrabadi MN. Extracting nuclear level density of 166Er using microscopic theory of interacting fermions. Nuclear Physics A. 2010;834(1):103c-6c.

[18] Nasri Nasrabadi M, editor Isospin dependence of nuclear level density of 28Al considering symmetry energy and pairing corrections. Journal of Physics Conference Series; 2011 May 01, 2011.

[19] Pahlavani MR, dinan MM. Retraction: Nuclear level density and thermal properties of 270110, 278112, and 290116 superheavy isotopes in low excitation energies. Canadian Journal of Physics. 2019;97:464-.

[20] Monga S, Kaur H. Semiclassical level density parameter with collective enhancements in nuclei. International Journal of Modern Physics E. 2021;30:2150020.

[21] Nasrabadi MN, Sepiani M, editors. Study of components and statistical reaction mechanism in simulation of nuclear process for optimized production of 64Cu and 67Ga medical radioisotopes using TALYS, EMPIRE and LISE++ nuclear reaction and evaporation codes. 4th International Congress in Advances in Applied Physics and Materials Science (APMAS 2014); 2015 March 01, 2015.

[22] Aydin A, Pekdogan H, Kaplan A, Sarpün İ, Tel E, Demir B. Comparison of level density models for the 60, 61, 62, 64 Ni (p, n) reactions of structural fusion material nickel from threshold to 30 MeV. Journal of Fusion Energy. 2015;34:1105-8.

[23] Kamal N, Nizam S, Aziz AA. The effects of nuclear level density model and alpha optical model potential to the excitation functions of novel therapeutic radionuclides. Applied Radiation and Isotopes. 2024;203:111085.

[24] Indira G, Anbalagan G. An investigation of the effects of optical model potentials and level density models on the calculation of excitation function for the production of medical isotopes 68 G e and 82 S r through alpha and proton induced nuclear reactions. Indian Journal of Physics. 2023:1-9.

[25] Schmitt C, Nadtochy P, Mazurek K. Fission as a relevant probe of the nuclear level density away from β-stability. Physics Letters B. 2023;840:137873.

[26] Nasri Nasrabadi M, Sepiani M. Study of nuclear level densities for exotic nuclei. Iranian Journal of Physics Research. 2019;12(1):67-75.

[27] Ignatyuk A, Weil J, Raman S, Kahane S. Density of discrete levels in Sn 116. Physical Review C. 1993;47(4):1504.

[28] Sepiani M, Nasrabadi M. Determination of nuclear level density based on a fully microscopic statistical partition function method for 58Ni. Journal of Physics G: Nuclear and Particle Physics. 2023;50(5):055103.

[29] Goriely S, Tondeur F, Pearson J. A Hartree–Fock nuclear mass table. Atomic Data and Nuclear Data Tables. 2001;77(2):311-81.

[30] Goriely S, Hilaire S, Koning AJ. Improved microscopic nuclear level densities within the Hartree-Fock-Bogoliubov plus combinatorial method. Physical Review C. 2008;78(6):064307.

[31] Goriely S. Global microscopic models for nuclear astrophysics applications. Nuclear Physics A. 2005;752:560-9.

[32] Nasrabadi MN, Sepiani M. Study of Collective Rotational Enhancement Factors for Nuclear Level Densities Using the Microscopic Theory of Interacting Fermions. Acta Physica Polonica B. 2014;45:1865.

[33] Alhassid Y, Bertsch GF, Gilbreth CN, Nakada H, Özen C, editors. Level densities of heavy nuclei in the shell model Monte Carlo approach. European Physical Journal Web of Conferences; 2016 June 01, 2016.

[34] W. Hauser, Feshbach H. The Inelastic Scattering of Neutrons. Physical Review. 1952;87.

[35] Hill DL, Wheeler JA. Nuclear constitution and the interpretation of fission phenomena. Physical Review. 1953;89(5):1102.

[36] Bohr Å. Conf. on Peaceful Uses of Atomic Energy. Geneva; 1955.

[37] Koning A, Hilaire S, Goriely S. TALYS: modeling of nuclear reactions. The European Physical Journal A. 2023;59(6):131.

[38] A. Koning, S. Hilaire, Goriely S. TALYS-1.96/2.0 Simulation of nuclear reactions, User Manual. 1.96/2.0 ed2021.

[39] Sepiani M, Nasrabadi M. Evidence on the high energy behavior of nuclear level density parameter. Physica Scripta. 2024;99(1):015302.

[40] Ignatyuk AV, Smirenkin GN, Tishin AS. Phenomenological description of energy dependence of the level density parameter. Yadernaya Fizika. 1975;21(3):485-90.

[41] Dwivedi NR, Monga S, Kaur H, Jain SR. Ignatyuk damping factor: A semiclassical formula. International Journal of Modern Physics E. 2019;28:1950061.

[42] Capote R, Herman M, Obložinský P, Young PG, Goriely S, Belgya T, et al. RIPL - Reference Input Parameter Library for Calculation of Nuclear Reactions and Nuclear Data Evaluations. Nuclear Data Sheets. 2009;110:3107-214.

[43] Romain P, Morillon B, Koning A. Neutron actinides evaluations with the TALYS code. NEMEA-3 Neutron Measurements, Evaluations and Applications. 2006;25:113.

[44] Dubrovina S, Shigin V, editors. Neutron Fission Cross Sections of Pa 231 and Pu 239 in the 1.5 to 1500 keV Energy Range. Soviet Physics Doklady; 1965.

[45] Fursov B, Samylin B, Smirenkin G. Fast neutron induced fission cross sections of 231Pa, 232U, 236U, and 243Am. Radiation Effects. 1986;93(1-4):305-8.

[46] Muir D, Veeser L, editors. Neutron-induced fission cross sections of 230Th and 231Pa. Proceedings of the 3rd Conference on Neutron Cross-Sections and Technology, Knoxville, TN; 1971.

[47] Oberstedt S, Oberstedt A, Hambsch F-J, Fritsch V, Lövestam G, Kornilov N. New results on the neutron-induced fission cross-section of 231Pa for incident neutron energies En= 0.8–3.5 MeV. Annals of Nuclear Energy. 2005;32(17):1867-74.

[48] Plattard S, Auchampaugh G, Hill N, De Saussure G, Harvey J, Perez R. Some Spectroscopic Properties of Fine Structures Observed near the Pa 231 (n, f) Fission Threshold. Physical Review Letters. 1981;46(10):633.

**How to cite this article**
M. Sepiani, M. Nasri Nasrabadi, *Analysis of the Microscopic Details and Components of the Nuclear Fission for Protactinium-231*, Journal of Nuclear Research and Applications (JONRA), Volume 4 Number 4 Autuam (2024) 1-10. **URL**: https://jonra.nstri.ir/article_1683.html, **DOI:** https:// doi.org/10.24200/jonra.2024.1630.1135.